Delivery date: July 2015

MODENA

Deliverable 1.3

Thermodynamic models

WP's leader: UniTS

Authors:

Joachim Gross
US
E-mail: gross@itt.uni-stuttgart.de

Jonas Mairhofer
US
E-mail: mairhofer@itt.uni-stuttgart.de

Principal investigators:
US: Joachim Gross, Jonas Mairhofer
UniTS: Sabrina Pricl, Erik Laurini

Project's coordinator:
Heinz Preisig, **NTNU** (N)

Contents

1 Objectives of the deliverable

The objective of deliverable 1.3 is to report on the thermodynamic models and their parameterization to calculate static properties, surface tensions and viscosities.

The report is organized as follows: the first section will introduce the equation of state (EOS) which is used in the MoDeNa project and explain its parameterization. The second section will cover the density functional theory (DFT) approach which is used to calculate surface tensions. In the third and fourth section, the results of surface tensions and viscosities are presented.

For both models (EOS and DFT) we present two approaches. Firstly, an approach on the level of components where parameters are determined for every type of molecule and, secondly, a group contribution (GC) approach where we assign parameters to each functional group making up the molecules.

Both approaches have their advantages and disadvantages. Parameterization on the component level usually leads to more accurate results. However, the parameterization has to be redone for every new component that is present in the system under study. GC methods on the other hand offer the flexibility that once the parameters of the functional groups that make up the molecules in the system are available, on adding new components of the same chemical family, i.e. consisting of the same functional groups, no new parameterization is needed. This can prove to be advantageous for the MoDeNa project as the components we are dealing with belong to a few chemical families (e.g. diols, diisocyanates). Therefore, once the parameters of the main chemical groups (e.g. -CH_2, -OH, -NCO, etc.) are known, adding further components of these families to the system does not require a new parameterization.

2 The PC-SAFT and GC-PC-SAFT equation of state

In the following section, the basic equations of the thermodynamic model to calculate static thermodynamic properties as well as viscosities, the PC-SAFT equation of state, and its group contribution version, GC-PC-SAFT, are presented.

The parameters of PC-SAFT and GC-PC-SAFT are the segment diameter σ, the segment number m and the dispersive interaction energy ϵ. To include interactions due to association two more parameters, the association energy and volume, ϵ_{AB} and κ_{AB}, respectively, are needed. Furthermore, to account for polar interactions, the dipol moment μ is used. For PC-SAFT, every component is characterized by a set of these parameters while for GC-PC-SAFT, every chemical group is assigned its own set of parameters.

The equations of PC-SAFT and its extensions to associating and polar components are taken from [1], [2] and [3]. Details on the GC-PC-SAFT EOS are taken from [4] and [5].

2.1 PC-SAFT

PC-SAFT is a molecular based EOS. Like all EOS from the SAFT (Statistical associating fluid theory [6] [7] [8]) family, its basic idea is to split the Helmholtz energy A into different contributions:

$$\frac{A}{NkT} = \frac{A^{IG}}{NkT} + \frac{A^{HC}}{NkT} + \frac{A^{Dispersion}}{NkT} + \frac{A^{Association}}{NkT} + \frac{A^{Polar}}{NkT} \tag{1}$$

where the single contributions of the ideal gas A^{IG}, volume exclusion and chain formation A^{HC} as well as dispersion, association and polar interactions, $A^{Dispersion}$, $A^{Association}$ and A^{Polar}, respectively, are calculated as:

$$\frac{A^{IG}}{NkT} = \sum_i x_i(ln(\rho_i) - 1) \tag{2}$$

with the mole fraction of component i x_i and the component density ρ_i.

$$\frac{A^{HC}}{NkT} = \bar{m}\frac{A^{HS}}{NkT} + \sum_i x_i(1 - m_i)ln(g_{ii}^{HS}) \tag{3}$$

where $\bar{m} = \sum_i x_i m_i$ and the contribution of volume exclusion is given by

$$\frac{A^{HS}}{NkT} = \frac{1}{\xi_0}\left[\frac{3\xi_1\xi_2}{1-\xi_3} + \frac{\xi_2^3}{\xi_3(1-\xi_3)^2} + \left(\frac{\xi_2^3}{\xi_3^2} - \xi_0\right) ln(1-\xi_3)\right] \tag{4}$$

with

$$\xi_n = \frac{\pi}{6}\rho\sum_i x_i m_i d_i^n \quad n \in (0,1,2,3)$$

the temperature dependent segment diameter

$$d_i(T) = \sigma_i \left[1 - 0.12exp\left(\frac{-3\epsilon_i}{kT}\right)\right]$$

and the radial distribution function of a hard sphere system

$$g_{ij}^{HS} = \frac{1}{1-\xi_3} + \left(\frac{d_i d_j}{d_i + d_j}\right)\frac{3\xi_2}{2(1-\xi_3)^2} + \left(\frac{d_i d_j}{d_i + d_j}\right)^2 \frac{\xi_2^2}{2(1-\xi_3)^3}$$

The dispersive contribution in equation 1 is calculated by a second order perturbation theory:

$$\frac{A^{Dispersion}}{NkT} = \frac{A_1}{NkT} + \frac{A_2}{NkT} \tag{5}$$

with the first and second order terms, A_1 and A_2, respectively:

$$\frac{A_1}{NkT} = -2\pi\rho I_1(\eta, \bar{m}) \sum_i \sum_j x_i x_j m_i m_j \left(\frac{\epsilon_{ij}}{kT}\right)\sigma_{ij}^3 \tag{6}$$

$$\frac{A_2}{NkT} = -\pi\rho\bar{m}\left(1 + Z^{HC} + \rho\frac{\partial Z^{HC}}{\partial\rho}\right)^{-1} I_2(\eta, \bar{m}) \sum_i \sum_j x_i x_j m_i m_j \left(\frac{\epsilon_{ij}}{kT}\right)^2 \sigma_{ij}^3 \tag{7}$$

The terms appearing in equations 6 and 7 can be calculated as $\sigma_{ij} = \frac{1}{2}(\sigma_i + \sigma_j)$ and $\epsilon_{ij} = \sqrt{\epsilon_i \epsilon_j}(1 - k_{ij})$ with the binary interaction parameter k_{ij} as well as

$$\left(1 + Z^{HC} + \rho\frac{\partial Z^{HC}}{\partial\rho}\right) = \left(1 + \bar{m}\frac{8\xi_3 - 2\xi_3^2}{(1-\xi_3)^4} + (1-\bar{m})\frac{20\xi_3 - 27\xi_3^2 + 12\xi_3^3 - 2\xi_3^4}{[(1-\xi_3)(2-\xi_3)]^2}\right)$$

$$I_1(\eta, \bar{m}) = \sum_{l=0}^{6} a_l(\bar{m})\eta^l$$

$$I_2(\eta, \bar{m}) = \sum_{l=0}^{6} b_l(\bar{m})\eta^l$$

$$a_l(\bar{m}) = a_{0l} + \frac{\bar{m}-1}{\bar{m}}a_{1l} + \frac{\bar{m}-1}{\bar{m}}\frac{\bar{m}-2}{\bar{m}}a_{2l}$$

$$b_l(\bar{m}) = b_{0l} + \frac{\bar{m}-1}{\bar{m}}b_{1l} + \frac{\bar{m}-1}{\bar{m}}\frac{\bar{m}-2}{\bar{m}}b_{2l}$$

with the packing fraction $\eta = \xi_3$ and the PC-SAFT model constants $a_{0l}, a_{1l}, a_{2l}, b_{0l}, b_{1l}, b_{2l} \quad l = (0, 1, 2, 3, 4, 5, 6)$ which can be found in [1].

The contribution to the Helmholtz energy due to association is given by

$$\frac{A^{Association}}{NkT} = \sum_i x_i \sum_{A_i}\left(lnX^{A_i} - \frac{X^{A_i}}{2} + \frac{1}{2}\right) \tag{8}$$

where X^{A_i} denotes the fraction of component i which is not bonded at its bonding site X^{A_i}:

$$X^{A_i} = \left(1 + \rho \sum_i x_i \sum_{B_j} X^{B_j} \Delta^{A_i B_j}\right)^{-1}$$

with

$$\Delta^{A_i B_j} = g_{ij}^{HS} \kappa^{A_i B_j} \sigma_{ij}^3 \left[exp\left(\frac{\epsilon^{A_i B_j}}{kT}\right) - 1\right]$$

The values of the association strength and volume of the mixture $\epsilon^{A_i B_j}$ and $\kappa^{A_i B_j}$, respectively, can be calculated from the pure component parameters as follows

$$\epsilon^{A_i B_j} = \frac{1}{2}\left(\epsilon^{A_i B_i} + \epsilon^{A_j B_j}\right)$$

$$\kappa^{A_i B_j} = \sqrt{\kappa^{A_i B_i} \kappa^{A_j B_j}} \left(\frac{2\sqrt{\sigma_{ii}\sigma_{jj}}}{\sigma_{ii} + \sigma_{jj}}\right)^3$$

The dipole term is given by

$$\frac{A^{Polar}}{NkT} = \frac{\tilde{a}_2^{dd}}{1 - \tilde{a}_3^{dd}/\tilde{a}_2^{dd}} \tag{9}$$

$$\tilde{a}_2^{dd} = -\pi\rho \sum_i \sum_j x_i x_j \frac{\epsilon_i}{kT} \frac{\epsilon_j}{kT} \frac{\sigma_i^3 \sigma_j^3}{\sigma_{ij}^3} \mu_i^{*2} \mu_j^{*2} J_2^{dd}$$

$$\tilde{a}_3^{dd} = -\frac{4\pi^2}{3} \rho^2 \sum_i \sum_j \sum_k x_i x_j x_k \frac{\epsilon_i}{kT} \frac{\epsilon_j}{kT} \frac{\epsilon_k}{kT} \frac{\sigma_i^3 \sigma_j^3 \sigma_k^3}{\sigma_{ij}\sigma_{ik}\sigma_{jk}} \mu_i^{*2} \mu_j^{*2} \mu_k^{*2} J_3^{dd}$$

$$J_2^{dd} = \sum_{n=0}^{4} \left(a_n(m_{ij}) + b_n(m_{ij}) \frac{\epsilon_{ij}}{kT}\right) \eta^n$$

$$J_3^{dd} = \sum_{n=0}^{4} c_n(m_{ijk}) \eta^n$$

$$\mu_i^{*2} = \frac{\mu_i^2}{m_i \sigma_i^3 \epsilon_i}$$

with $m_{ij} = (m_i m_j)^{1/2}$ and $m_{ijk} = (m_i m_j m_k)^{1/3}$.

Once the Helmholtz energy A has been obtained by equation 1, other thermodynamic properites can be calculated from derivatives of A, e.g. pressure $p = -\left(\frac{\partial A}{\partial V}\right)_{T,N}$ and chemical potentials $\mu_i = \left(\frac{\partial A}{\partial N_i}\right)_{T,V}$.

2.2 GC-PC-SAFT

2.2.1 Homosegmented GC-PC-SAFT

In the homosegmented GC-PC-SAFT approach, the pure component parameters are obtained from the parameters of the single functional groups in the given component as:

$$
\begin{aligned}
m_i &= \sum_\alpha n_{i,\alpha} m_{i,\alpha} \\
m_i \sigma_i^3 &= \sum_\alpha n_{i,\alpha} m_{i,\alpha} \sigma_{i,\alpha}^3 \\
m_i \epsilon_i &= \sum_\alpha n_{i,\alpha} m_{i,\alpha} \epsilon_{i,\alpha} \\
\mu_i^2 &= \sum_\alpha n_{i,\alpha} \mu_{i,\alpha}^2
\end{aligned}
$$

where α runs over the different types of functional groups in component i and $n_{i,\alpha}$ indicates how many times a given group is present in component i. Furthermore, $m_{i,\alpha}$, $\sigma_{i,\alpha}$, $\epsilon_{i,\alpha}$ and $\mu_{i,\alpha}$ are the group specific EOS parameters.
The values of the association strength and volume of component i, ϵ^{AiBi} and κ^{AiBi}, respectively, are set to the values of the functional group that causes the association. Once the pure component parameters have been calculated, the regular PC-SAFT equations are used, see chapter .

2.2.2 Heterosegmented GC-PC-SAFT

In the heterosegmented GC-PC-SAFT approach, the equations for the different contributions to the Helmholtz energy are no longer formulated on the component level but on the level of the single functional groups in the component.

The contribution due to chain formation and volume exclusion now reads

$$
\frac{A^{HC}}{NkT} = \bar{m}\frac{A^{HS}}{NkT} - \sum_i x_i(m_i - 1) \sum_\alpha \sum_\beta B_{i\alpha i\beta} ln g^{HS}_{i\alpha i\beta}(d_{i\alpha i\beta}) \tag{10}
$$

In equation 10, the first sum runs over all components in the system, while the second and third sum run over all types of groups of every component i. The segment number of component i m_i is calculated from the segment numbers of the single groups as $m_i = \sum_\alpha n_{i,\alpha} m_{i,\alpha}$ and the average segment number of the mixture is obtained as $\bar{m} = \sum_i x_i m_i$. The contribution due to volume exclusion A^{HS} can still be obtained from equation 4. Furthermore, the temperature dependent segment diameter $d_{i\alpha i\beta}$ and the segment level radial distribution function $g^{HS}_{i\alpha i\beta}(d_{i\alpha i\beta})$ are

$$
d_{i\alpha} = \sigma_{i\alpha}\left(1 - 0.12 exp\left(\frac{-3\epsilon_{i\alpha}}{kT}\right)\right)
$$

and

$$g^{HS}_{i\alpha i\beta}(d_{i\alpha i\beta}) = \frac{1}{1-\xi_3} + \left(\frac{d_{i\alpha}d_{i\beta}}{d_{i\alpha}+d_{i\beta}}\right)\frac{3\xi_2}{(1-\xi_3)^2} + \left(\frac{d_{i\alpha}d_{i\beta}}{d_{i\alpha}+d_{i\beta}}\right)^2\frac{2\xi_2^2}{(1-\xi_3)^3}$$

with

$$\xi_n = \frac{\pi}{6}\rho\sum_i x_i m_i \sum_\alpha z_{i\alpha} d^n_{i\alpha} \quad n = (0,1,2,3)$$

$$z_{i,\alpha} = n_{i,\alpha}\frac{m_{i,\alpha}}{m_i}$$

The matrix $B_{i\alpha i\beta}$ stores information about the structure of the molecule by counting the bonds between functional groups of type α and β in component i.
The first and second order terms of the dispersive contribution for the heterosegmented GC-PC-SAFT EOS are

$$\frac{A_1}{NkT} = -2\pi\rho I_1(\bar{m},\eta)\sum_i\sum_j x_i x_j m_i m_j \sum_\alpha\sum_\beta z_{i\alpha} z_{i\beta}\left(\frac{\epsilon_{i\alpha i\beta}}{kT}\right)\sigma^3_{i\alpha i\beta} \tag{11}$$

and

$$\frac{A_2}{NkT} = -\pi\rho\bar{m}\left(1 + Z^{HC} + \rho\frac{\partial Z^{HC}}{\partial\rho}\right)^{-1} I_2(\bar{m},\eta)\sum_i\sum_j x_i x_j m_i m_j \sum_\alpha\sum_\beta z_{i\alpha} z_{i\beta}\left(\frac{\epsilon_{i\alpha i\beta}}{kT}\right)^2\sigma^3_{i\alpha i\beta} \tag{12}$$

where the single terms appearing in equations 11 and 12 can be calculated as described in chapter as well as $\epsilon_{i\alpha i\beta} = \sqrt{\epsilon_{i\alpha}\epsilon_{i\beta}}$ and $\sigma_{i\alpha i\beta} = 0.5\,(\sigma_{i\alpha} + \sigma_{i\beta})$.

$$\frac{A^{Association}}{NkT} = \sum_i x_i \sum_\alpha n_{i\alpha}\sum_{Ai\alpha} N_{i\alpha}\left(lnX^{Ai\alpha} - \frac{1-X^{Ai\alpha}}{2}\right) \tag{13}$$

$$X^{Ai\alpha} = \left(1 + \rho\sum_j x_j\sum_\beta n_{i\beta}\sum_{Bj\beta} N_{j\beta}X^{Bj\beta}\Delta^{Ai\alpha Bj\beta}\right)^{-1}$$

$$\Delta^{Ai\alpha Bj\beta} = g_{i\alpha j\beta}(d_{i\alpha j\beta})\kappa^{Ai\alpha Bj\beta}\sigma^3_{i\alpha j\beta}\left(exp\left(\frac{\epsilon^{Ai\alpha Bj\beta}}{kT}\right) - 1\right)$$

$$\epsilon^{Ai\alpha Bj\beta} = 0.5\left(\epsilon^{Ai\alpha Bi\alpha} + \epsilon^{Aj\beta Bj\beta}\right)$$

$$\kappa^{Ai\alpha Bj\beta} = \sqrt{\kappa^{Ai\alpha Bi\alpha}\kappa^{Aj\beta Bj\beta}}\left(\frac{\sqrt{\sigma_{i\alpha i\alpha}\sigma_{j\beta j\beta}}}{1/2\left(\sigma_{i\alpha i\alpha+\sigma_{j\beta j\beta}}\right)}\right)^3$$

where the third sum in equation 13 runs over all association sites A on segments of type α and $N_{i\alpha}$ represents the number of association sites of a certain type.
Polar contributions can be calculated analogous to the homosegmented case, equation 9, using the same relation to obtain the pure component dipole moment from the group values as for the homosegmented case, see section .

2.3 Parameterization of PC-SAFT

2.3.1 Parameterization using experimental data

In cases where there is succifient experimental data available, the EOS parameters can be obtained by a fitting procedure which usually takes the residuals of calculated and experimental values of liquid densities and vapor pressures as objective function. The following table shows the values of the PC-SAFT parameters obtained by fitting to experimentel data for components which are relevant to the MODENA project for example as monomers and chain extenders of the PU polymer or as physical or chemical blowing agents.

Component	MW /g/mol	m/MW	ϵ/k /K	$\sigma/\AA$	ϵ_{AB}/k/K	κ_{AB}	μ /Debye
1,2-Ethandiol	62.07	0.04209	310.114	3.154	2711.659	0.03	2.410
1,3-Propandiol	76.09	0.03321	247.561	3.424	3834.694	0.03	2.551
1,4-Butandiol	90.12	0.04598	199.009	3.085	4078.174	0.03	3.927
1,5-Pentandiol	104.15	0.04402	137.996	3.001	5630.302	0.03	2.371
1,6-Hexandiol	118.17	0.03406	248.156	3.485	3776.660	0.03	2.500
1,10-Decandiol	174.28	0.03994	256.764	3.369	32452.261	0.03	2.143
Tripropylene Glycol	192.25	0.01239	148.678	4.549	5597.844	0.03	0.41
Tetrahydrofuran	72.11	0.03433	274.134	3.512	-	-	1.631
4,4'-MDI	250.26	0.03077	283.053	2.886	-	-	-
2,4-TDI	174.16	0.02667	297.632	3.523	-	-	2.521
CO_2	44.01	0.03438	163.333	3.187	-	-	4.400
Pentane	72.15	0.03728	231.197	3.773	-	-	-
Cylopentane	70.13	0.03373	265.829	3.711	-	-	-

with molecular mass MW, segment number m, the energy of the dispersive interactions ϵ, the segment diameter σ, the energy of associative interactions ϵ_{AB}, the association volume κ_{AB} the dipole moment μ and Boltzmann's constant k.
As a validation of the results obtained for those components where experimental data is available, the following table shows the dimensionless average absolute deviation (AAD%) of the calculated from the experimental results for values of liquid density and vapor pressure. Both properties can be reproduced with only small deviations from the experimental values.

Component	AAD% p^{vap}	AAD% ρ^{liq}
1,2-Ethandiol	1.80	0.28
1,3-Propandiol	3.63	0.78
1,4-Butandiol	3.21	0.41
1,5-Pentandiol	4.96	1.52
1,6-Hexandiol	4.29	0.15
1,10-Decandiol	0.70	0.19
Tripropylene Glycol	1.77	1.13
Tetrahydrofuran	0.50	0.27
4,4'-MDI	1.53	0.28
2,4-TDI	1.09	0.09
CO_2	0.22	0.22
Pentane	0.23	0.31
Cylopentane	0.83	0.74

2.3.2 Parameterization using data from molecular simulations

For the polyurethane poylmers, experimental data which could be used to obtain the PC-SAFT parameters is scarce. Therefore, a different approach is tried here and molecular dynamics (MD) simultions are performed in order to generate results which in turn are used to fit the EOS parameters against. Because pressure values fluctuate widely in these simulations, besides values of liquid density the heat of evaporation is used instead of the vapor pressure as the second property in the fitting routine.

In the following, we give a brief outline of the simulation set up. In order to obtain the heat of evaporation, simulations of corresponding gas and liquid phases have to be performed. The liquid phase simulations are carried out as MD simulations in the NpT-ensemble, i.e. with a constant number of particles and fixed values of pressure and temperature. The corresponding gas phase is simulated using stochastic dynamics (SD) in the NVT-ensemble, i.e. with a constant number of particles and fixed values of volume and temperature. In SD simulations the Langevin equations of motion instead of Newton's equations of motion are integrated to obtain the trajectories of the molecules. Langevin equations of motion include an additional friction coefficient and a stochastic force. These modifications speed up the gas phase simulations considerably because they instantly account for processes which otherise would be apparent only on much longer time scales due to the lack of interactions of the particles in the gas phase.
From these simulations, the heat of evaporation $\Delta^{lv}h$ can be obtained as

$$\Delta^{lv}h = h^v - h^l = u^v - u^l + RT - pv^l \tag{14}$$

with enthalpy h, potential energy of the system u, universal gas constant R, temperature T, pressure p and specific volume v. The superscripts l and v denote properties of the liquid and gas phase, respectively. In equation 14 we applied the ideal gas law to the gas phase, i.e. $pv^v = RT$.
All properties needed to calculate $\Delta^{lv}h$ are obtained by averaging the values at certain time steps over the complete simulation time. This procedure is carried out for different temperatures to obtain enough data to fit the PC-SAFT parameters.

As a general test of the applicability of this method, the EOS parameters of hexatriacontane are calculated from results of liquid density and heat of evaporation of molecular dynamic simulations with the GROMOS 54 A7 [9] [10] force field. With these parameters we then calculate the solubility of methane in hexatriacontane with the PC-SAFT EOS and compare the results to experimental values taken from [11].
As figure 1 shows, the simulation results are in good agreement with the experimental values, especially at low pressures and higher temperatures.

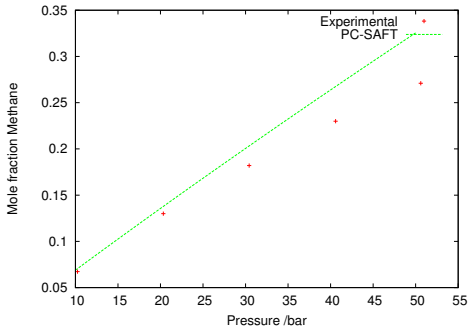

(a) T=373.15K

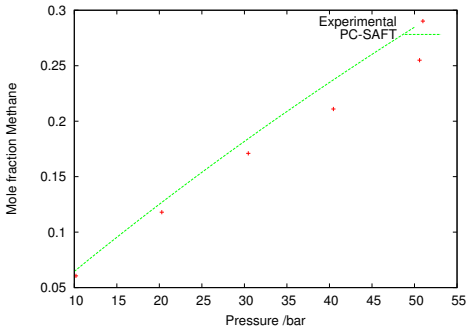

(b) T=473.15K

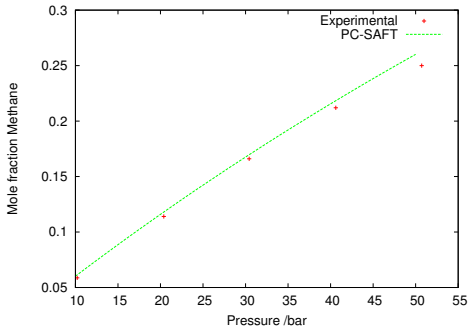

(c) T=573.15K

Figure 1: Experimental results [11] and results of PC-SAFT calculations for the solubility of methane in hexatriacontane as a function of pressure at three different temperatures. The EOS parameters of hexatriacontane are fit against values of liquid densities and heat of evaporation obtained in molecular dynamic simulations.

Therefore, using data from molecular simulations can be seen as a valid alternative to calculate the EOS parameters of components where experimental data is not available.

2.4 Parameterization of GC-PC-SAFT

For GC-PC-SAFT, the EOS parameters have to be determined for every functional group. For a wide range of groups this has been done in prior studies [5] and these values are applied unchanged where applicable. For the components relevant to the MoDeNa project, the cyanate-group (-N=C=O) for the diisocyanates and the hydroxyl-group (-O-H) for the diols are parameterized.

In order to obtain the parameters for the hydroxy-group, experimental data of a group of diols consisting of 190 data points of liquid densities and vapor pressures for the components 1-4-Butandiol, 1-5-Pentandiol, 1-6-Hexandiol, 1-7-Heptandiol, 1-8-Octandiol, 1-9-Nonandiol, 1-10-Decandiol as well as Tripropylene glycol (TPG) are used. For the cyanate-group, 129 experimental data points of 1-4-Diisocyanatobutane, 1-6-Diisocyanatohexane, 1-8-Diisocyanatooctane and 4-4'-MDI are used.

Group	m	ϵ/k /K	$\sigma/\AA$	ϵ_{AB}/k/K	κ_{AB}	μ /Debye
-OH	0.07057	2055.03	5.757	4611.22	0.968E-03	-
-NCO	1.03960	374.68	3.851	-	-	

With these parameters, liquid densities and vapor pressures of the diols can be reproduced with an avergae absolute deviation of AAD% $p^{vap}_{diols} = 16.35$ and AAD% $\rho^{liq}_{diols} = 4.73$. For the diisocyanates these figures are AAD% $p^{vap}_{diiso} = 41.61$ and AAD% $\rho^{liq}_{diiso} = 14.38$.

3 Density Functional Theory

In the following sections we will present three different density functional theory (DFT) approaches. Approach one and two are both compatible to PC-SAFT and differ only in the way they treat dispersive contributions. Approach three is a group-contribution method and it is compatible to heterosegment GC-PC-SAFT EOS.

The basic idea of DFT is that the equilibrium density profile in an inhomogeneous system minimizes the grandcanonical potential Ω, i.e.

$$\left(\frac{\delta\Omega}{\delta\rho(\boldsymbol{r})}\right)_{\rho(\boldsymbol{r})=\rho_{equilibrium}(\boldsymbol{r})} = 0 \tag{15}$$

with $\Omega = A[\rho(\boldsymbol{r})] - \int \sum_i \rho_i(\boldsymbol{r})\mu_i d\boldsymbol{r}$
The Helmholtz energy A, which is now a functional of the density profile, is again split into separate contributions

$$\frac{A}{kT} = \frac{A^{IG}}{kT} + \frac{A^{HS}}{kT} + \frac{A^{Chain}}{kT} + \frac{A^{Dispersion}}{kT} + \frac{A^{Association}}{kT} + \frac{A^{Polar}}{kT} \tag{16}$$

3.1 DFT based on PC-SAFT

For the DFT based on PC-SAFT, the terms in equation 16 are presented in the following section [12] [13].
The ideal gas contribution reads

$$\frac{A^{IG}[\rho]}{kT} = \int \rho(\boldsymbol{r})\,(ln(\rho(\boldsymbol{r})-1)\,d\boldsymbol{r} \tag{17}$$

The hard sphere contribution is calculated using the weighted densities of the fundamental measure theory [14] [15]

$$\frac{A^{HS}[\rho]}{kT} = \int \Phi(\{n_\alpha\})d\boldsymbol{r} \tag{18}$$

with the local hard sphere Hemlholtz energy density Φ

$$\Phi(n_\alpha) = -n_0 ln(1-n_3) + \frac{n_1 n_2 - \vec{n}_1\vec{n}_2}{1-n_3} + (n_2^3 - 3n_2\vec{n}_2\vec{n}_2)\frac{n_3 + (1-n_3)^2 ln(1-n_3)}{36\pi n_3^2(1-n_3)^2}$$

which depends on the weighted densities n_α

$$n_\alpha(\boldsymbol{r}) = \sum_{i=1} \int \rho_i(\boldsymbol{r}-\boldsymbol{r'})\omega_\alpha^i(\boldsymbol{r'})d\boldsymbol{r'}$$

that can be calculated using the following weight functions

$$\begin{aligned}
\omega_3^i(\boldsymbol{r}) &= \Theta(\frac{\sigma_i}{2} - r)\\
\omega_2^i(\boldsymbol{r}) &= \delta(\frac{\sigma_i}{2} - r)\\
\omega_1^i(\boldsymbol{r}) &= \frac{\omega_i^2(r)}{2\pi\sigma_i}\\
\omega_0^i(\boldsymbol{r}) &= \frac{\omega_i^2(r)}{\pi\sigma_i^2}\\
\vec{\omega}_2^i(\boldsymbol{r}) &= \frac{\boldsymbol{r}}{r}\delta(\frac{\sigma_i}{2} - r)\\
\vec{\omega}_1^i(\boldsymbol{r}) &= \frac{\vec{\omega}_2^i(\boldsymbol{r})}{2\pi\sigma_i}
\end{aligned}$$

where $r = |\boldsymbol{r}|$.
The contribution due to chain formation can be calculated as

$$\frac{A^{Chain}[\rho]}{kT} = \sum_i \int (m_i - 1)\,\rho_i(\boldsymbol{r})\left(ln\left(\frac{\rho_i(\boldsymbol{r})}{y^{dd}(\bar{\rho}_i(\boldsymbol{r}))\lambda_i(\boldsymbol{r})}\right)\right)d\boldsymbol{r} \tag{19}$$

with the cavity correlatoin function y^{dd}

$$y^{dd}(\bar{\rho}_i(\boldsymbol{r})) = \bar{g}_{ii}^{HS}(\bar{\rho}_i(\boldsymbol{r}))$$

$$\bar{g}_{ij}^{HS}(\bar{\rho}_i(\boldsymbol{r})) = \frac{1}{1-\bar{\xi}_3(\boldsymbol{r})} + \left(\frac{d_i d_j}{d_i+d_j}\right)\frac{3\bar{\xi}_2(\boldsymbol{r})}{2(1-\bar{\xi}_3(\boldsymbol{r}))^2} + \left(\frac{d_i d_j}{d_i+d_j}\right)^2 \frac{\bar{\xi}_2^2(\boldsymbol{r})}{2(1-\bar{\xi}_3(\boldsymbol{r}))^3}$$

and

$$\begin{aligned}
\lambda_i(\boldsymbol{r}) &= \frac{1}{4\pi d_i^2}\int \rho_i(\boldsymbol{r})\delta(d_i - |\boldsymbol{r}-\boldsymbol{r'}|)d\boldsymbol{r} \\
\bar{\xi}_n(\boldsymbol{r}) &= \frac{\pi}{6}\sum_i \bar{\rho}_i(\boldsymbol{r}) m_i d_i^n \quad n \in (0,1,2,3) \\
\bar{\rho}_i(\boldsymbol{r}) &= \frac{3}{4\pi d_i^3}\int \rho_i(\boldsymbol{r'})\Theta(d_i - |\boldsymbol{r}-\boldsymbol{r'}|)d\boldsymbol{r'}
\end{aligned}$$

The first order term of the dispersive contribution is given by

$$\frac{A^{1PT}[\rho]}{kT} = \frac{1}{2}\pi\sum_i\sum_j m_i m_j \int\int \rho_i(\boldsymbol{r})\rho_j(\boldsymbol{r'})\left(\frac{u^{PT}(\hat{r})}{kT}\right) g^{HC}(\hat{r},\hat{\rho})d\boldsymbol{r'}d\boldsymbol{r} \tag{20}$$

whith $\hat{r} = |\boldsymbol{r}-\boldsymbol{r'}|$ and $\hat{\rho} = \frac{1}{2}\sum_i(\rho_i(\boldsymbol{r}) + \rho_i(\boldsymbol{r'}))$. u^{PT} denotes the Lennard-Jones potential that is used to describe the disperive interations and g^{HC} is the radial distribution function of a hard chain fluid.
Equation 20 is not yet compatible to PC-SAFT. This can be achieved easily, however, by a small local adjustment, see [12].
For approach one of the PC-SAFT based DFT, dispersive interactions are treated by evaluating equation 20. The drawback of this method is the time consuming task of carrying out the integration which requires the recalculation of g^{HC} and u^{PT} for many values of $\hat{r}$. Therefore, approach two treats the dispersive contribution in a weighted density approximation which is defined as

$$\frac{A^{Dispersion}[\rho]}{kT} = \int \bar{\rho}^*(\boldsymbol{r})\frac{A^{Dispersion}(\bar{\rho}^*(\boldsymbol{r}))}{NkT}d\boldsymbol{r} \tag{21}$$

$$\bar{\rho}^*(\boldsymbol{r}) = \sum_i \frac{3}{4\pi\sigma_{Disp,i}^3}\int \rho_i(\boldsymbol{r'})\Theta(\sigma_{Disp,i} - |\boldsymbol{r}-\boldsymbol{r'}|)d\boldsymbol{r'}$$

where $\frac{A^{Dispersion}(\bar{\rho}^*(\boldsymbol{r}))}{NkT}$ is obtained by evaluating the bulk EOS, equation 5, at the local weighted density $\bar{\rho}^*(\boldsymbol{r})$.

Associative and polar interactions are treated in a local density approximation in both approaches, i.e.

$$\frac{A^{Association}[\rho]}{kT} = \int \rho(\boldsymbol{r})\frac{A^{Association}(\rho(\boldsymbol{r}))}{NkT}d\boldsymbol{r} \tag{22}$$

and

$$\frac{A^{Polar}[\rho]}{kT} = \int \rho(\boldsymbol{r}) \frac{A^{Polar}(\rho(\boldsymbol{r}))}{NkT} d\boldsymbol{r} \tag{23}$$

where $\frac{A^{Association}(\rho(\boldsymbol{r}))}{NkT}$ and $\frac{A^{Polar}(\rho(\boldsymbol{r}))}{NkT}$ are obtained by evaluating the bulk EOS, equations 8 and 9, at the local density $\rho(\boldsymbol{r})$.

3.2 DFT based on heterosegmented GC-PC-SAFT

In this section, a DFT which is compatible to the heterosegment GC-PC-SAFT EOS is presented. So far, contributions of volume exclusion, chain formation and dispersion are implemented. Besides the dispersive contribution of heterosegment GC-PC-SAFT EOS it uses the chain formation term of modified iSAFT [16].
The main equation to calculate the density profile of segment is in a system where no external potential is present is [16]

$$\rho_{is}^{seg}(\mathbf{r}) = exp\left(\beta\mu_M\right) exp\left(D_{is}(\mathbf{r})\right) I_{1,is}(\mathbf{r}) I_{2,is}(\mathbf{r}) \tag{24}$$

with the bulk chemical potential of the chain molecule that segment is belongs to μ_M, $\beta = \frac{1}{kT}$ and

$$\begin{aligned}
I_{1,1}(\mathbf{r}) &= 1 \\
I_{1,js}(\mathbf{r}) &= \int I_{1,js-1}(\mathbf{r'}) exp\left(D_{js-1}(\mathbf{r'})\right) \Delta^{js-1,js}(\mathbf{r'},\mathbf{r}) d\mathbf{r'} \\
I_{2,NS_j}(\mathbf{r}) &= 1 \\
I_{2,js}(\mathbf{r}) &= \int I_{2,js+1}(\mathbf{r'}) exp\left(D_{js+1}(\mathbf{r'})\right) \Delta^{js,js+1}(\mathbf{r'},\mathbf{r}) d\mathbf{r'}
\end{aligned}$$

where NS_j is the number of functional groups on the chain molecule that group js belongs to. Furthermore,

$$D_\alpha(\mathbf{r}) = \frac{1}{2} \sum_{\gamma}^{NS} \sum_{\gamma'}^{\{\gamma'\}} \int \rho_\gamma^{seg}(\mathbf{r}_1) \frac{\delta ln y_{contact}^{\gamma\gamma'}\left[\{\bar{\rho}_\alpha^{seg}(\mathbf{r}_1)\}, (\mathbf{r},\mathbf{r}_1)\right]}{\delta\rho_\alpha^{seg}} d\mathbf{r}_1 - \frac{\delta\beta A^{HS}}{\delta\rho_\alpha^{seg}(\mathbf{r})} - \frac{\delta\beta A^{Dispersion}}{\delta\rho_\alpha^{seg}(\mathbf{r})} \tag{25}$$

$$\bar{\rho}_\alpha^{seg}(\boldsymbol{r}) = \frac{3}{4\pi\sigma_\alpha^3}\int \rho_\alpha^{seg}(\boldsymbol{r'})\Theta(\sigma_\alpha - |\boldsymbol{r}-\boldsymbol{r'}|)d\boldsymbol{r'}$$

$$y_{contact}^{\gamma\gamma'}\left[\{\bar{\rho}_\alpha^{seg}(\mathbf{r}_1)\},(\mathbf{r},\mathbf{r}_1)\right] = \left(y_{contact}^{\gamma\gamma'}\left[\{\bar{\rho}_\alpha^{seg}(\mathbf{r})\}\right]\cdot y_{contact}^{\gamma\gamma'}\left[\{\bar{\rho}_\alpha^{seg}(\mathbf{r}_1)\}\right]\right)^{0.5}$$

$$y_{contact}^{\gamma\gamma'}\left[\{\bar{\rho}_\alpha^{seg}(\mathbf{r})\}\right] = \frac{1}{1-\bar{\xi}_3} + \frac{\sigma_\gamma\sigma_{\gamma'}}{\sigma_\gamma+\sigma_{\gamma'}}\frac{\bar{\xi}_2}{(1-\bar{\xi}_3)^2} + 2\left(\frac{\sigma_\gamma\sigma_{\gamma'}}{\sigma_\gamma+\sigma_{\gamma'}}\right)^2\frac{\bar{\xi}_2^2}{(1-\bar{\xi}_3)^3}$$

$$\bar{\xi}_n = \frac{\pi}{6}\sum_\gamma^{NS} m_\gamma \bar{\rho}_\gamma^{seg}(\mathbf{r})\sigma_\gamma^n$$

$$\Delta^{\gamma,\gamma'}(\mathbf{r'},\mathbf{r}) = \frac{\delta\left(|\mathbf{r'}-\mathbf{r}|-\sigma^{\gamma\gamma'}\right)}{4\pi\left(\sigma^{\gamma\gamma'}\right)^2}y_{contact}^{\gamma\gamma'}(\mathbf{r},\mathbf{r'})$$

where NS in equation 25 is the total number of groups, i.e. $\mathrm{NS} = \sum_i \mathrm{NS}_i$.
The hard sphere contribution $\frac{A^{HS}}{kT}$ is calculated according to equation 18 with the small modification, that the weighted densities are multiplied by the group segment number m_γ, i.e. $n_\alpha(\boldsymbol{r}) = \sum_\gamma^{NS} m_\gamma \int \rho_\gamma^{seg}(\boldsymbol{r}-\boldsymbol{r'})\omega_\alpha^\gamma(\boldsymbol{r'})d\boldsymbol{r'}$.

$\frac{A^{Dispersion}}{kT}$ is calculated with a weighted density approximation according to

$$\frac{A^{Dispersion}[\rho]}{kT} = \int \bar{\rho}^*(\boldsymbol{r})\frac{A^{Dispersion,GC-PC-SAFT}(\bar{\rho}^*(\boldsymbol{r}))}{NkT}d\boldsymbol{r} \tag{26}$$

$$\bar{\rho}^*(\boldsymbol{r}) = \sum_i \bar{\rho}_i^*(\boldsymbol{r})$$

$$\bar{\rho}_i^*(\boldsymbol{r}) = \frac{1}{NS_i}\sum_{is}^{NS_i}\bar{\rho}_{is}^*(\boldsymbol{r})$$

$$\bar{\rho}_{is}^*(\boldsymbol{r}) = \frac{3}{4\pi\sigma_{Disp,is}^3}\int \rho_{is}(\boldsymbol{r'})\Theta(\sigma_{Disp,is}-|\boldsymbol{r}-\boldsymbol{r'}|)d\boldsymbol{r'}$$

where $\frac{A^{Dispersion,GC-PC-SAFT}(\bar{\rho}^*(\boldsymbol{r}))}{NkT}$ is calculated as

$$\frac{A^{Dispersion,GC-PC-SAFT}(\bar{\rho}^*(\boldsymbol{r}))}{NkT} = \frac{A_1^{Disp}}{NkT} + \frac{A_2^{Disp}}{NkT} \tag{27}$$

with

$$\frac{A_1^{Disp}}{NkT} = -2\pi\bar{\rho}^* I_1(\bar{m},\bar{\eta})\sum_i\sum_j x_i x_j \sum_{is}^{NS_i}\sum_{js}^{NS_j} m_{is}m_{js}\omega_{is}\omega_{js}\frac{\epsilon_{isjs}}{kT}\sigma_{isjs}^3$$

$$\frac{A_2^{Disp}}{NkT} = -\pi\bar{\rho}^*\bar{m}I_2(\bar{m},\bar{\eta})\left(1+Z^{hc}+\rho\frac{\partial Z^{hc}}{\partial\rho}\right)^{-1}\sum_i\sum_j x_i x_j \sum_{is}^{NS_i}\sum_{js}^{NS_j} m_{is}m_{js}\omega_{is}\omega_{js}\left(\frac{\epsilon_{isjs}}{kT}\right)^2\sigma_{isjs}^3$$

and $\bar{\eta} = \bar{\xi}_3$, $\bar{m} = \sum_i x_i \sum_{is}^{NS,i} m_{is}$ as well as $\omega_{is} = \frac{\bar{\rho}^*_{is}}{\bar{\rho}^*_i}$ where $\bar{\rho}^*_i$ is the weighted density of the chain molecule that segment is belongs to.

4 Surface Tension

In the first part of this section, results obtained with the group contribution DFT are compared to experimental values and results of the PC-SAFT based DFT approaches in order to validate the group contribution DFT. In the second part, systems relevant to the MoDeNa project are studied. So far, the group contribution DFT is not able to treat ring molecules such as cyclopentane or 44-MDI. Therefore, it is not applied to the systems studied in the second part of this section.

The advantage of the group contribution DFT approach is that is yields results on a more detailed level. Figure 2 shows the density profiles obtained from a simulation of pentane. While the PC-SAFT based DFT approaches can only claculate the total density of pentane, the group contribution DFT also provides the density profiles of the five chemical groups of pentane seperately. From figure 2 is is apparent that the profiles of the single groups differ in the interface. The value of this additional information for a simple pentane simulation is small, however, for more complex molecules with strong polar or associative groups and surfactants, the knowledge of the group density profiles may prove important.

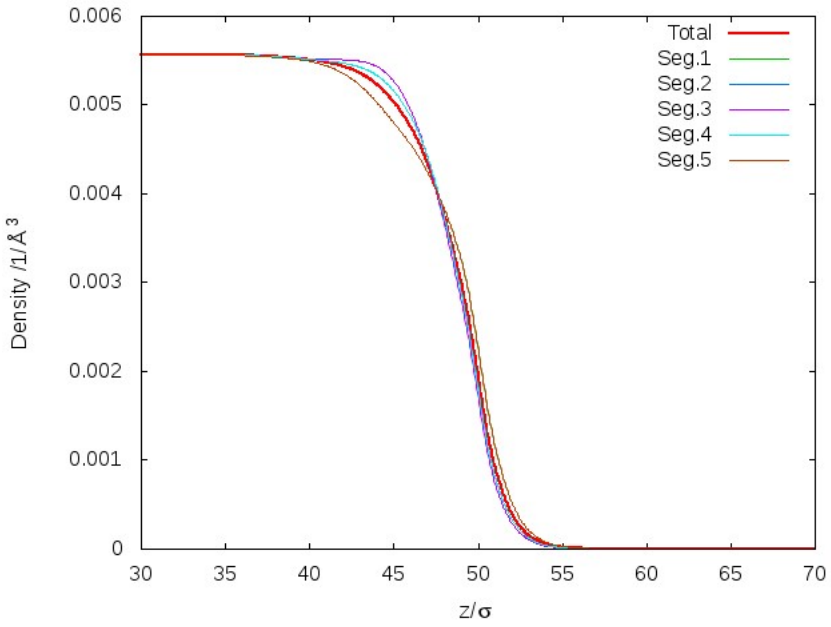

Figure 2: Segment densities and total density of pentane at T=233.15K calculated with the group contribution DFT.

Figures 3, 4 and 5 compare the simulation results of the different DFT approaches to experimental data. For pure components, figure 3, the PC-SAFT based approaches perform comparably well, while deviations to experimental data are a little larger for the

group contribution DFT, especially for larger molecules.

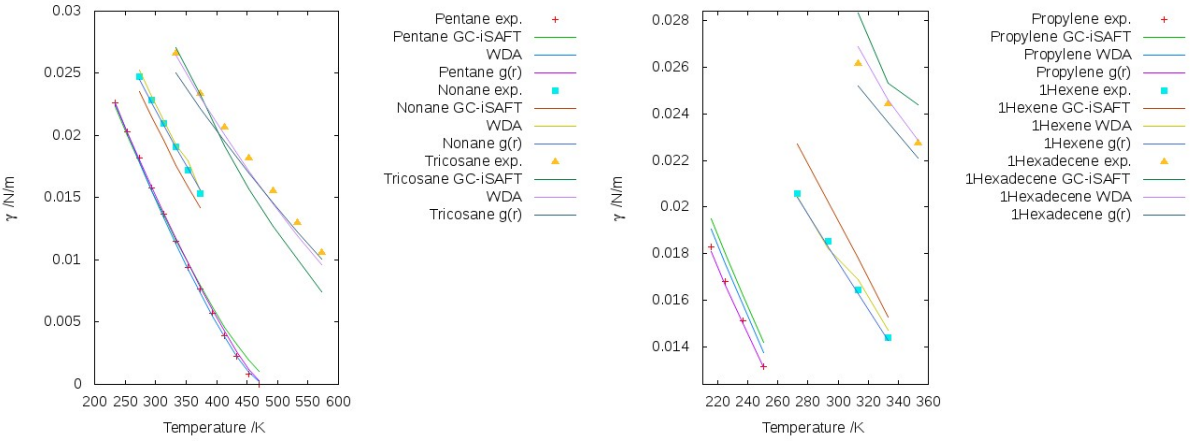

Figure 3: Values of surface tension of alkanes and alkenes calculated with all three DFT approaches (here *g(r)* ≡ *approach 1*, *WDA* ≡ *approach 2* and *GC-iSAFT* ≡ *approach 3*).

However, for the binary mixtures shown in figure 4 the group contribution method performs a little better than the other two methods. The situation for the three component mixture in figure 5 is similar. Only the group contribution method and the weighted density approach are capable of calculating results for ternary mixtures. While neither method matches the experiments perfectly, the group contribution method is in better agreement with the experiments over the complete calculated pressure range. Figure 5 (b) shows the density profiles of all three components obtained with these two DFT approaches. The profiles agree qualitatively, i.e. both methods predict an accumluation of nitrogen and butane at the interface.
From these results it can be confirmed that the group contribution DFT gives reliable results and, therefore, it will be further extended in order to treat additional classes of substances such as ring molecules.

In the remaining part of this section, the PC-SAFT based DFT approaches are applied to systems containing components which are present in the MoDeNa project. Figure 6 shows simulation and experimental results of cyclopentane and 44-MDI as a function of temperature. Both DFT methods show a similar behaviour for both components. In both cases, the results of approach one are in better agreement with the experiments.
Figure 7 shows results for the binary mixtures of CO_2 with butandiol, THF and 44-MDI as a function of temperature. For the mixtures containing butandiol and THF, both DFT methods exhibit very similar results. The larger deviations for the mixture CO_2 and 44-MDI can be attributed to poor convegence of approach one (denoted *g(r)*).
Similar convergence problems arise for approach one for the systems shown in figure 8. The displayed results are obtained for a binary mixture consisting of a dimer of 44-MDI and butandiol and pentane (a), cyclopentane (b) as well as CO_2 (c).
The results of this section show that from the PC-SAFT based approaches, when convergence can be achieved, approach one is more accurate than approach two. However, approach one is limited to pure components and binary mixtures. Therefore, approach

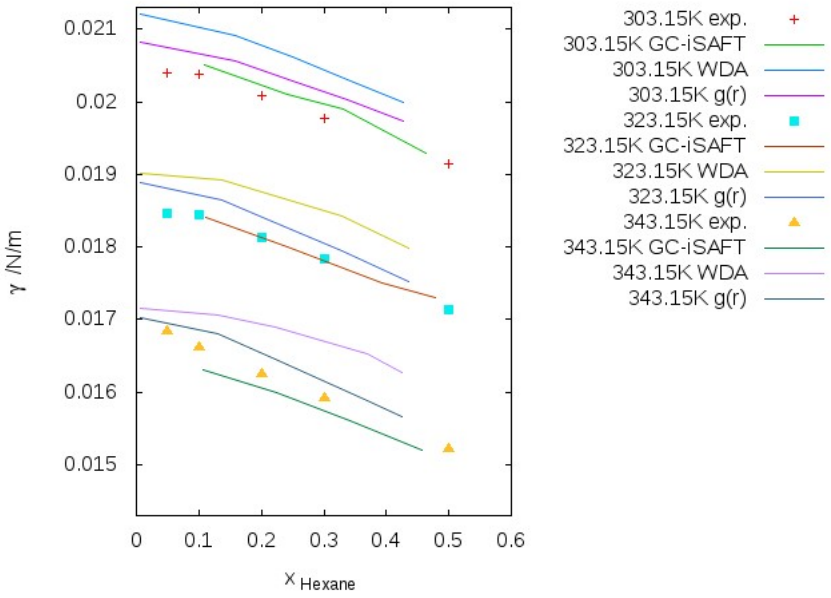

Figure 4: Surface tension of a hexane-octane mixture as a function of the molar fraction of Hexane in the liquid phase (here *g(r)* ≡ *approach 1*, *WDA* ≡ *approach 2* and *GC-iSAFT* ≡ *approach 3*).

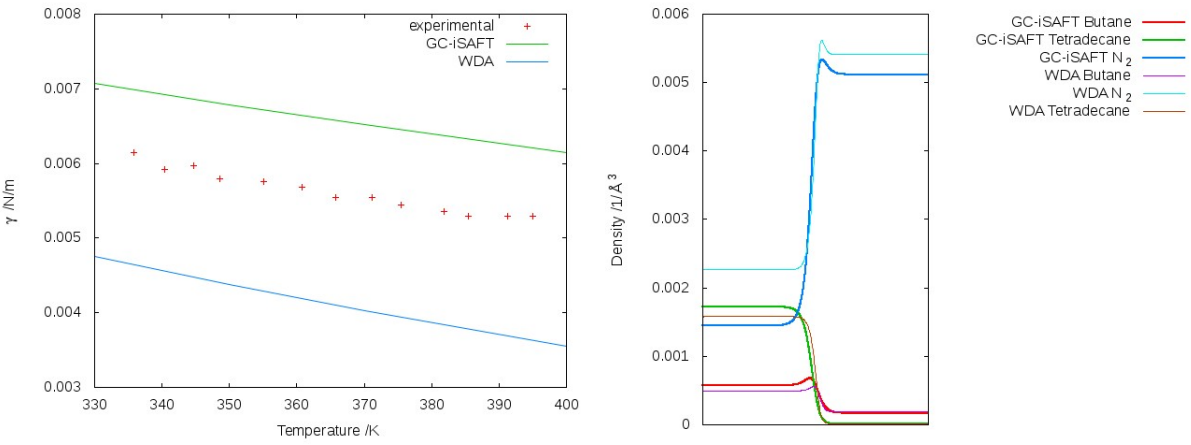

Figure 5: Left: Values of surface tension of a nitrogen, butane, tetradecane mixture as a function of pressure at T=373.15K. Right: density profiles calculated with approach two (*WDA*) and three (*GC-iSAFT*) at p=330bar and T=373.15K.

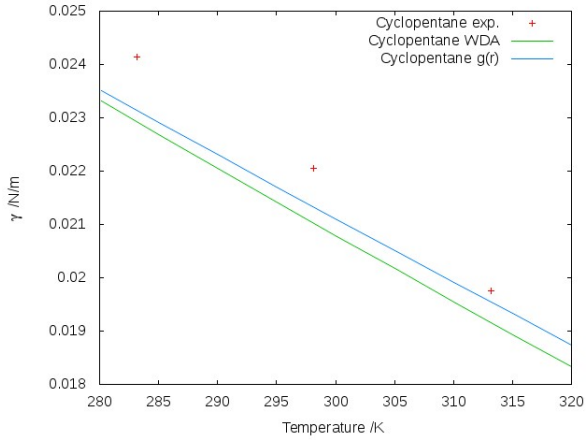

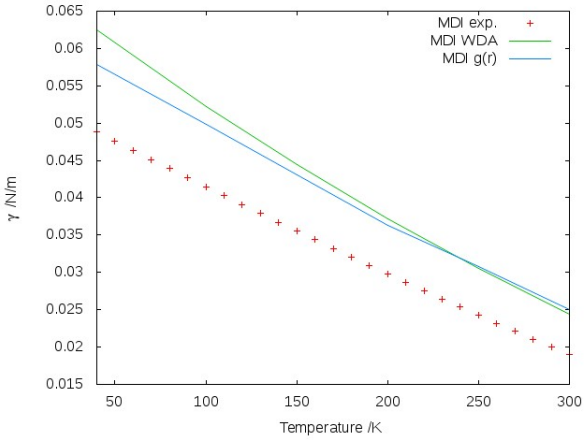

Figure 6: Surface tension of Cyclopentane and 4-4'-MDI calculated with approach one (*g(r)*) and two (*WDA*) as a function of temperature.

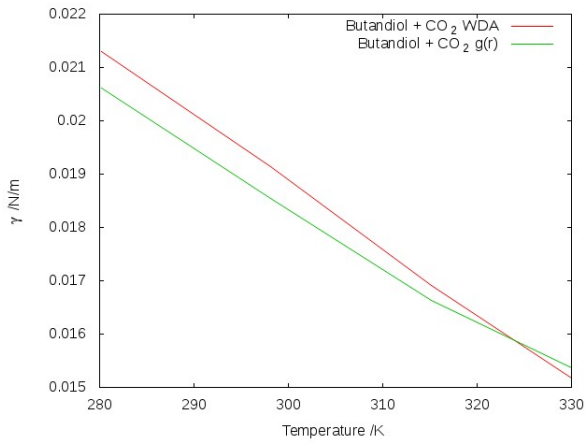

(a) Surface tension Butandiol and CO_2.

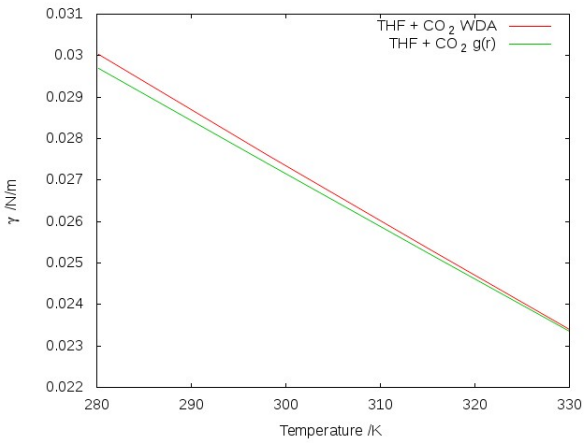

(b) Surface tension THF and CO_2.

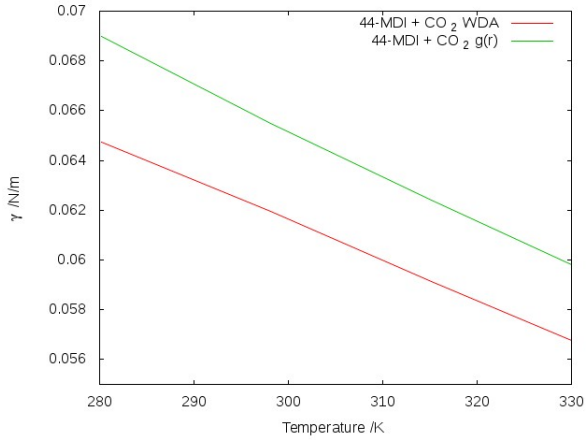

(c) Surface tension 44-MDI and CO_2.

Figure 7: Surface tension of Butandiol (a), THF (b) and 44-MDI (c) in mixtures with CO_2 as functions of temperature with approach one (*g(r)*) and two (*WDA*).

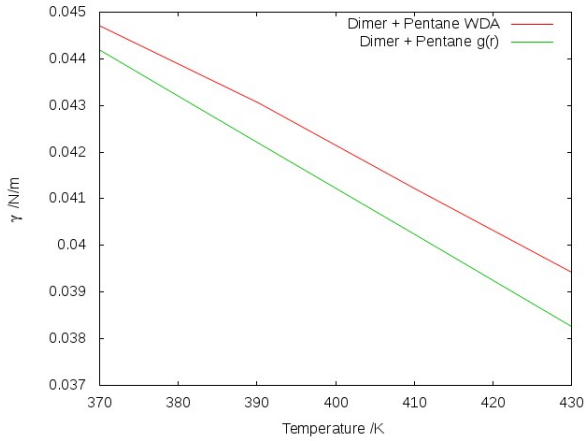

(a) Surface tension of dimer and Pentane.

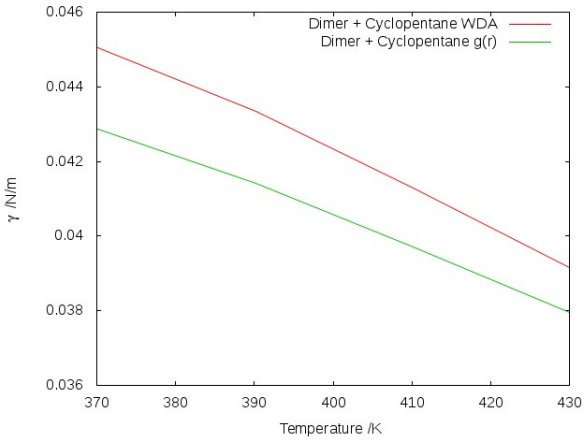

(b) Surface tension of dimer and Cyclopentane.

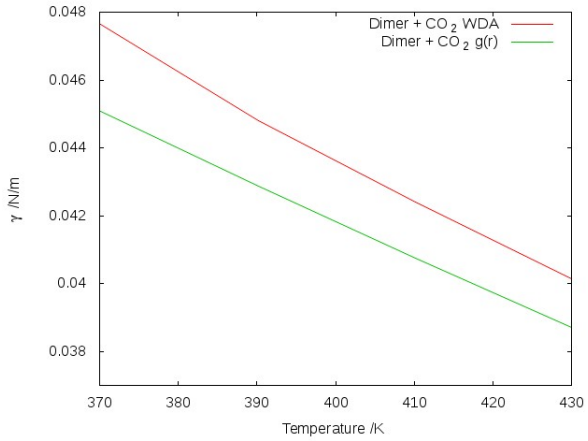

(c) Surface tension of dimer and CO_2.

Figure 8: Surface tension of a 44-MDI-Butandiol-dimer and Pentane (a), Cyclopentane (b) and CO_2 (c) calculated with with approach one ($g(r)$) and two (WDA).

2 seems advantageous for the MoDeNa project. The group contribution DFT showed larger deviations from experiments than the PC-SAFT based DFT approaches for pure components but better agreement for mixtures and, furthermore, since it is based on a group contribution method, it is more flexible and therefore more suited for MoDeNa than the PC-SAFT based DFT approaches.

5 Viscosities

Viscosities are calculated using an entropy-scaling approach by Rosenfeld [17] [18] and its implementation with (GC)-PC-SAFT by Lötgering-Lin and Gross [19].
The basic idea of this approach is that the reduced viscosity $\eta*$ is a monovariable function of the residual entropy s_{res}. Where the reduced viscosity is defined as

$$\eta* = \frac{\eta}{\eta_{CE}} \tag{28}$$

where η_{CE} is the Chapman-Enskog viscosity defined as

$$\eta_{CE} = \frac{5}{16}\frac{\sqrt{MkT/(m_i N_A \pi)}}{\sigma_i^2 \Omega^{(2,2)*}}$$

Here, $\Omega^{(2,2)*}$ denotes the reduced collision integral. An empirical approximation is used to calculate the value of $\Omega^{(2,2)*}$ [20]. And furthermore, M denotes molar mass, k is the Boltzmann constant, Avogradros number N_A and the pure component parameters m_i and σ_i which for the implementation with GC-PC-SAFT are calculated from the group parameters using the relations given in chapter .
The residual entropy is defined as the difference to the ideal gas entropy as $s_{res}(\rho, T) = s(\rho, T) - s^{IG}(\rho, T)$ and it is calculated with (GC)-PC-SAFT as $s_{res}(\rho, T) = -\left(\frac{\partial(A_{res}/N)}{\partial T}\right)_\rho$.
The empirical correlation to calculate pure component viscosities is

$$ln\eta_i* = A_i + B_i z + C_i z^2 + D_i z^3 \tag{29}$$

where $z = \frac{s_{res}}{km_i}$.
For the PC-SAFT version, the parameters A_i, B_i, C_i and D_i are adjusted to experimental viscosities of component i by a least-squares fit. For GC-PC-SAFT, the parameters are first determined for the single groups and in a second step calculated for a pure component i by the following relations:

$$A_i = \sum_\alpha n_{i,\alpha} m_\alpha \sigma_\alpha^3 A_\alpha$$

$$B_i = \sum_\alpha \frac{n_{i,\alpha} m_\alpha \sigma_\alpha^3}{V_{tot,i}^\gamma} B_\alpha$$

$$C_i = \sum_\alpha n_{i,\alpha} C_\alpha$$

$$D_i = D \sum_\alpha n_{i,\alpha}$$

where $n_{i,\alpha}$ is defined as in chapter , $V_{tot,i} = \sum_\alpha n_{i,\alpha} m_\alpha \sigma_\alpha^3$ and the model constants $\gamma = 0.45$ and $D = -0.01245$.

For the PC-SAFT approach, the four model parameters are fitted to 9 data points for Tripropylene glycol (TPG), 76 data points for 1-4-Butandiol (BD) and 6 data points for 4-4'-MDI.
For the GC-PC-SAFT version, the parameters for the functional groups -OH and -O- are fitted to 242 data points of a group of diols consisting of 1-4-Butandiol, 1-5-Pentandiol, 1-6-Hexandiol, 1-7-Heptandiol, 1-8-Octandiol, 1-9-Nonandiol, 1-10-Decandiol and TPG. Furthermore, the parameters for the functional group -NCO are fitted to 27 data points of a group of diisocynates consisting of 1-4-Diisocyanatobutane, 1-6-Diisocyanatohexane, 1-8-Diisocyanatooctane and 4-4'-MDI.
The remaining functional groups such as $-CH_2, -CH_3$, etc. have been fitted in earlier studies [19] to extensive experimental data and are applied unchanged to the diols and diisocyanates of the MoDeNa project.
The following table shows the mean absolute relative deviations (MAD) between simulation and experimental viscosity values for both approaches.

	MAD % PC-SAFT	MAD % GC-PC-SAFT
TPG	2.12	4.55
BD	3.66	12.19
MDI	1.13	5.50

Figures 9, 10 and 11 show the simulation as well as the experimental results. Since s_{res} is a calculated property that depends on the used EOS, values of s_{res} differ for the PC-SAFT and the GC-PC-SAFT approach for a given state point. Also, since the Chapman-Enskog viscosity η_{CE} is calculated from the EOS parameters m and σ which have different values for a given component in the PC-SAFT and the GC-PC-SAFT approach, the x and y axes of plots of the same component are not identical.

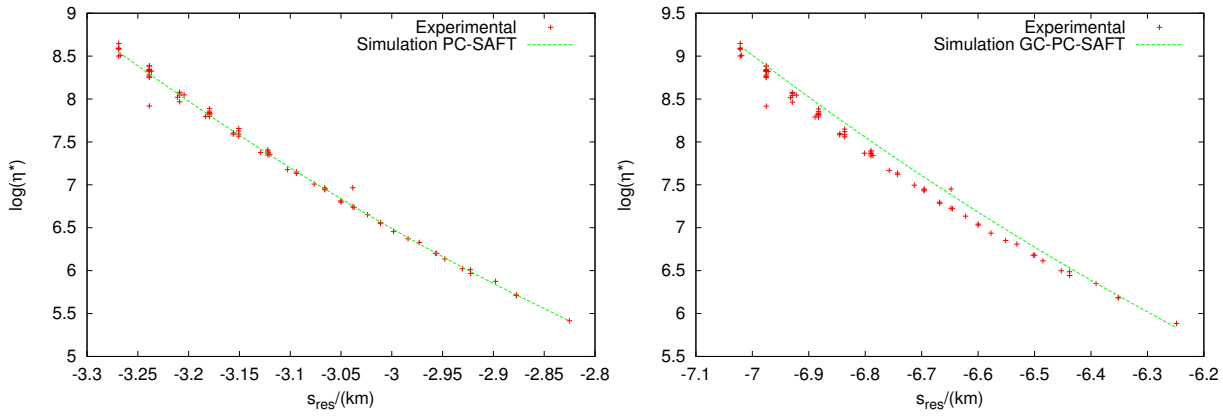

Figure 9: Calculated and experimental viscosities of 1-4-Butandiol. Left: Results of PC-SAFT. Right: Results of GC-PC-SAFT.

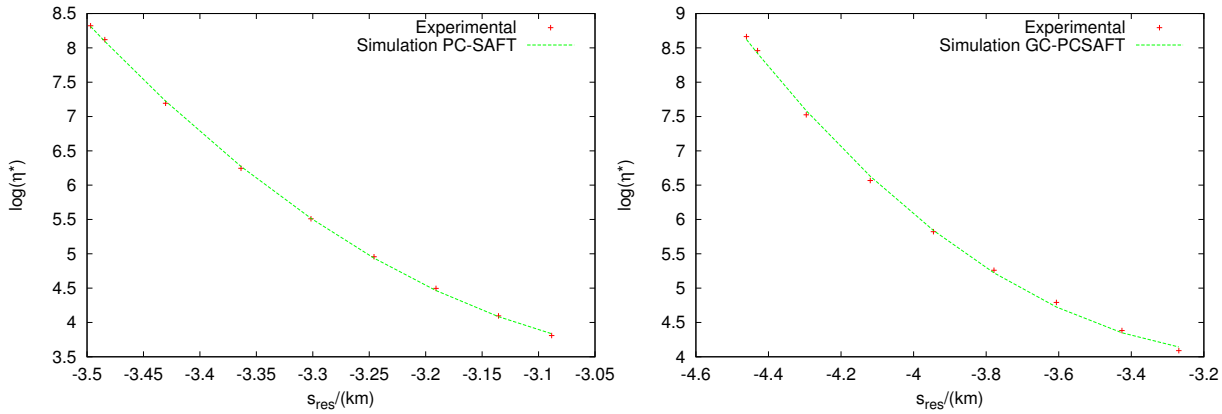

Figure 10: Calculated and experimental viscosities of TPG. Left: Results of PC-SAFT. Right: Results of GC-PC-SAFT.

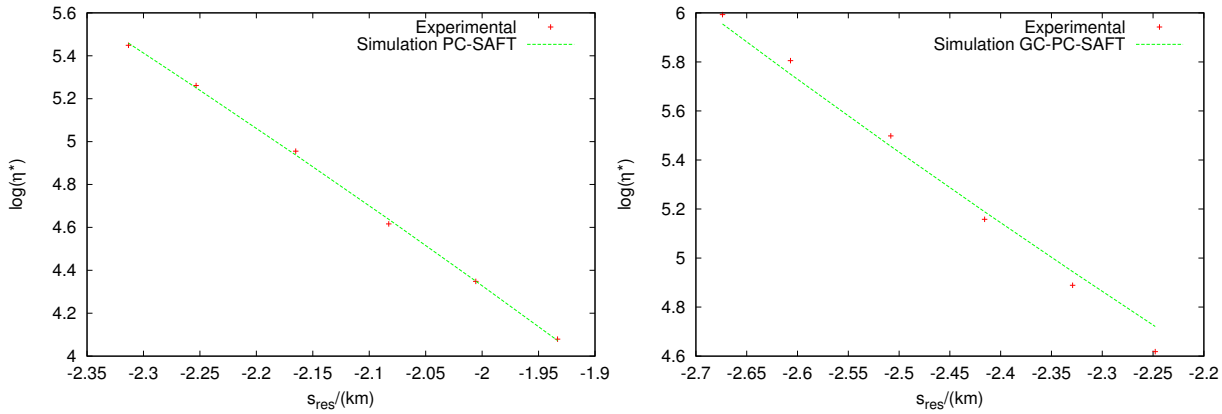

Figure 11: Calculated and experimental viscosities of 4-4'-MDI. Left: Results of PC-SAFT. Right: Results of GC-PC-SAFT.

6 Force field optimization

US has conducted an optimization of the van der Waals parameters of the force field selected by UNITS in task 1.2. The objective of the optimization is the accurate representation of vapor-liquid equilibria, i.e. the densities of the coexisting liquid and vapor phase as well as vapor pressures. The fundamentals of the optimization procedure are presented in the work of Hemmen et al. [21].
Figure 12 and 13 show the improvement in the calculation of the phase envelope and vapor pressure curve of methylisocyanate during the single steps of the optimization. In these simulations, the van der Waals parameters of the atoms of the cyanate group are adjusted to experimental data.

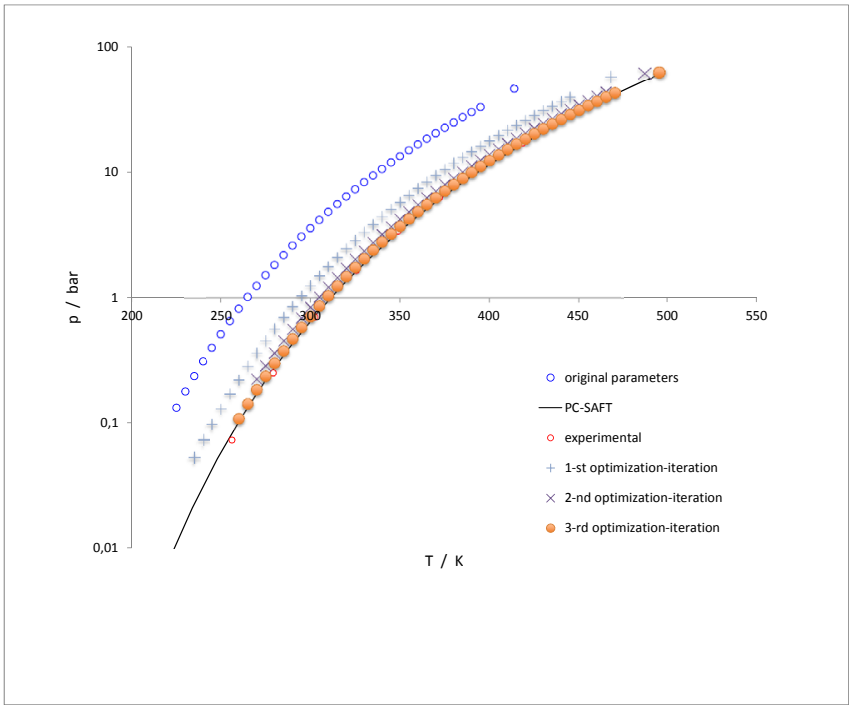

Figure 12: Monte Carlo simulation results of vapor pressure for methylisocyanate for the single optimization iterations of the adjustment of the van der Waals parameters of the cyanate group atoms. The solid curve denotes PC-SAFT results with parameters which were adjusted to the depicted experimental data and indicate the final trend of the Monte Carlo results with optimized parameters.

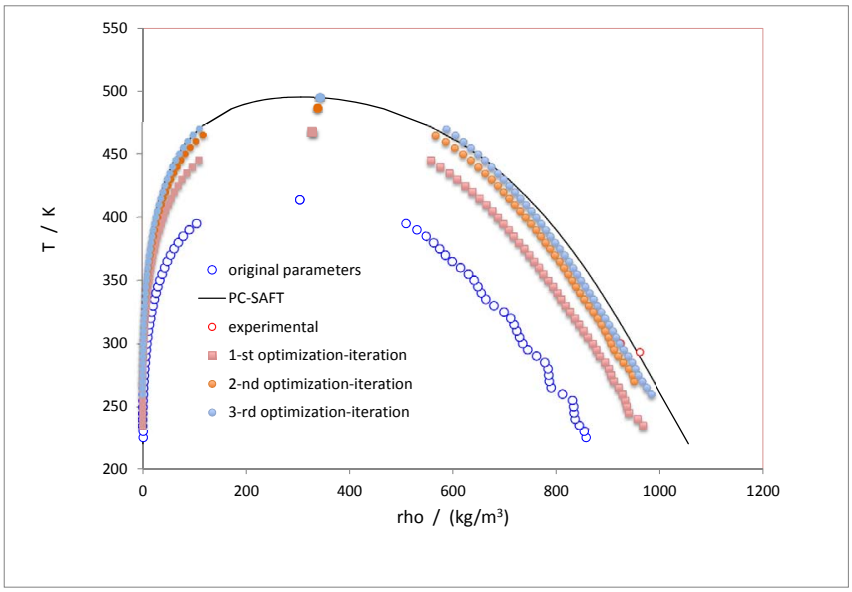

Figure 13: Monte Carlo simulation results of the densities for the corresponding vapor and liquid phases in equilibrium of methylisocyanate for the single optimization iterations of the adjustment of the van der Waals parameters of the cyanate group atoms. The solid curve denotes PC-SAFT results with parameters which were adjusted to the depicted experimental data and indicate the final trend of the Monte Carlo results with optimized parameters.

However, as reported by UNITS in milestone 1.2, the original values of the force field parameters resulted in very accurate results for structural properties. Since the calculation of these structural properties and not the determination of phase equilibria is the main purpose of the atomistic simulations in the MoDeNa project, the original parameter values will be used unchanged in subsequent molecular simulations.

7 Summary and Outlook

The PC-SAFT EOS and its group contribution version GC-PC-SAFT as well as DFT approaches based on PC-SAFT and also on GC-PC-SAFT are presented.
In general, the agreement between simulation and experimental results is better for PC-SAFT based approaches. Exceptions include results of surface tension of binary and ternary mixtures where results of the group contributino method are in better agreement with experiments.
Viscosities are calculated by an entropy scaling approach with good agreement between simulation and experimental results for most components. Surface tensions can be reproduced with acceptable deviations from experiments for most systems. However, in some simulations convergence problems occur.

Next steps will include the integration of the viscosity model into the MoDeNa framework, i.e. the identification of suitable surrogate models as well as extending the GC-PC-SAFT based DFT approach to components with more complex interactions and ring molecules.

References

[1] J. Gross and G. Sadowski, "Perturbed-chain saft: An equation of state based on a perturbation theory for chain molecules," *Industrial & Engineering Chemistry Research*, vol. 40, no. 4, pp. 1244–1260, 2001.

[2] J. Gross and G. Sadowski, "Application of the perturbed-chain saft equation of state to associating systems," *Industrial & Engineering Chemistry Research*, vol. 41, no. 22, pp. 5510–5515, 2002.

[3] J. Gross and J. Vrabec, "An equation-of-state contribution for polar components: Dipolar molecules," *AIChE Journal*, vol. 52, no. 3, pp. 1194–1204, 2006.

[4] J. Gross, O. Spuhl, F. Tumakaka, and G. Sadowski, "Modeling copolymer systems using the perturbed-chain saft equation of state," *Industrial & Engineering Chemistry Research*, vol. 42, no. 6, pp. 1266–1274, 2003.

[5] E. Sauer, M. Stavrou, and J. Gross, "Comparison between a homo- and a heterosegmented group contribution approach based on the perturbed-chain polar statistical associating fluid theory equation of state," *Industrial & Engineering Chemistry Research*, vol. 53, no. 38, pp. 14854–14864, 2014.

[6] W. Chapman, K. Gubbins, G. Jackson, and M. Radosz, "Saft: Equation-of-state solution model for associating fluids," *Fluid Phase Equilibria*, vol. 52, no. 0, pp. 31 – 38, 1989.

[7] W. Chapman, K. Gubbins, C. Joslin, and C. Gray, "Theory and simulation of associating liquid mixtures," *Fluid Phase Equilibria*, vol. 29, no. 0, pp. 337 – 346, 1986.

[8] C. Joslin, C. Gray, W. Chapman, and K. Gubbins, "Theory and simulation of associating liquid mixtures. ii," *Molecular Physics*, vol. 62, no. 4, pp. 843–860, 1987.

[9] W. R. P. Scott, P. H. Huenenberger, I. G. Tironi, A. E. Mark, S. R. Billeter, J. Fennen, A. E. Torda, T. Huber, P. Krueger, and W. F. van Gunsteren, "The gromos biomolecular simulation program package," *The Journal of Physical Chemistry A*, vol. 103, no. 19, pp. 3596–3607, 1999.

[10] N. Schmid, A. Eichenberger, A. Choutko, S. Riniker, M. Winger, A. Mark, and W. van Gunsteren, "Definition and testing of the gromos force-field versions 54a7 and 54b7," *European Biophysics Journal*, vol. 40, no. 7, pp. 843–856, 2011.

[11] F. N. Tsai, S. H. Huang, H. M. Lin, and K. C. Chao, "Solubility of methane, ethane, and carbon dioxide in n-hexatriacontane," *Journal of Chemical & Engineering Data*, vol. 32, no. 4, pp. 467–469, 1987.

[12] J. Gross, "A density functional theory for vapor-liquid interfaces using the pcp-saft equation of state," *The Journal of Chemical Physics*, vol. 131, no. 20, pp. –, 2009.

[13] C. Klink and J. Gross, "A density functional theory for vapor-liquid interfaces of mixtures using the perturbed-chain polar statistical associating fluid theory equation of state," *Industrial & Engineering Chemistry Research*, vol. 53, no. 14, pp. 6169–6178, 2014.

[14] Y. Rosenfeld, "Free-energy model for the inhomogeneous hard-sphere fluid mixture and density-functional theory of freezing," *Phys. Rev. Lett.*, vol. 63, pp. 980–983, Aug 1989.

[15] R. Roth, R. Evans, A. Lang, and G. Kahl, "Fundamental measure theory for hard-sphere mixtures revisited: the white bear version," *Journal of Physics: Condensed Matter*, vol. 14, no. 46, p. 12063, 2002.

[16] S. Jain, A. Dominik, and W. G. Chapman, "Modified interfacial statistical associating fluid theory: A perturbation density functional theory for inhomogeneous complex fluids," *The Journal of Chemical Physics*, vol. 127, no. 24, pp. –, 2007.

[17] Y. Rosenfeld, "Relation between the transport coefficients and the internal entropy of simple systems," *Phys. Rev. A*, vol. 15, pp. 2545–2549, Jun 1977.

[18] Y. Rosenfeld, "A quasi-universal scaling law for atomic transport in simple fluids," *Journal of Physics: Condensed Matter*, vol. 11, no. 28, p. 5415, 1999.

[19] O. Loetgering-Lin and J. Gross, "Group contribution method for viscosities based on entropy scaling using the perturbed-chain polar statistical associating fluid theory," *Industrial & Engineering Chemistry Research*, vol. 54, no. 32, pp. 7942–7952, 2015.

[20] P. D. Neufeld, A. Janzen, and R. Aziz, "Empirical equations to calculate 16 of the transport collision integrals ω (l, s)* for the lennard-jones (12–6) potential," *The Journal of Chemical Physics*, vol. 57, no. 3, pp. 1100–1102, 1972.

[21] A. Hemmen, A. Z. Panagiotopoulos, and J. Gross, "Grand canonical monte carlo simulations guided by an analytic equation of state - transferable anisotropic mie potentials for ethers," *The Journal of Physical Chemistry B*, vol. 119, no. 23, pp. 7087–7099, 2015.